

## Structural and magnetic etch damage in CoFeB

L. Kraye, J. W. Lau, and B. J. Kirby

Citation: *Journal of Applied Physics* **115**, 17B751 (2014); doi: 10.1063/1.4869276

View online: <http://dx.doi.org/10.1063/1.4869276>

View Table of Contents: <http://scitation.aip.org/content/aip/journal/jap/115/17?ver=pdfcov>

Published by the [AIP Publishing](#)

---

### Articles you may be interested in

[Measurement of magnetization using domain compressibility in CoFeB films with perpendicular anisotropy](#)  
*Appl. Phys. Lett.* **104**, 122404 (2014); 10.1063/1.4869482

[Effect of Mg interlayer on perpendicular magnetic anisotropy of CoFeB films in MgO/Mg/CoFeB/Ta structure](#)  
*Appl. Phys. Lett.* **101**, 122414 (2012); 10.1063/1.4754118

[Chemical diffusion: Another factor affecting the magnetoresistance ratio in Ta/CoFeB/MgO/CoFeB/Ta magnetic tunnel junction](#)  
*Appl. Phys. Lett.* **101**, 012406 (2012); 10.1063/1.4732463

[Effect of thickness of MgO, Co-Fe-B, and Ta layers on perpendicular magnetic anisotropy of \[Ta/Co<sub>60</sub>Fe<sub>20</sub>B<sub>20</sub>/MgO\]<sub>5</sub> multilayered films](#)  
*J. Appl. Phys.* **111**, 07C111 (2012); 10.1063/1.3673408

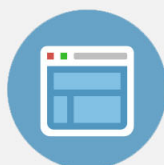
[Transmission electron microscopy investigation of CoFeB/MgO/CoFeB pseudospin valves annealed at different temperatures](#)  
*J. Appl. Phys.* **106**, 023920 (2009); 10.1063/1.3182817

---

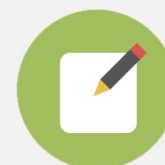


## Re-register for Table of Content Alerts

Create a profile.



Sign up today!



## Structural and magnetic etch damage in CoFeB

L. Kraye<sup>1,2</sup>, J. W. Lau,<sup>3</sup> and B. J. Kirby<sup>4,a)</sup>

<sup>1</sup>Physics Department, University of California, San Diego, California 92093, USA

<sup>2</sup>Electrical and Computer Engineering Department, University of Maryland, College Park, Maryland 20742, USA

<sup>3</sup>Materials Science and Engineering Division, NIST, Gaithersburg, Maryland 20899, USA

<sup>4</sup>Center for Neutron Research, NIST, Gaithersburg, Maryland 20899, USA

(Presented 7 November 2013; received 25 September 2013; accepted 14 October 2013; published online 26 March 2014)

A detailed understanding of the interfacial properties of thin films used in magnetic media is critical for the aggressive component scaling required for continued improvement in storage density. In particular, it is important to understand how common etching and milling processes affect the interfacial magnetism. We have used polarized neutron reflectometry and transmission electron microscopy to characterize the structural and magnetic properties of an ion beam etched interface of a CoFeB film. We found that the etching process results in a sharp magnetic interface buried under a nanometer scale layer of non-magnetic, compositionally distinct material. © 2014 AIP Publishing LLC. [<http://dx.doi.org/10.1063/1.4869276>]

### I. INTRODUCTION

The areal density of magnetic hard drives has increased at an annual rate greater than 25% for most of the past 50 years, largely through aggressive scaling of the components—most notably the thin film heads. Continued improvement will require precise sub-nanometer scale optimization. Of particular interest is the understanding and control of magnetic interfaces created during device processing by etching and milling. It is well known that etching and capping can alter the microstructure, electronic, and magnetic properties of the interface, resulting in drastic changes to the net magnetic properties. As dimensions of devices become smaller, such effects become progressively more important. However, the exact nature of such magnetically degraded, or “dead,” layers is not well understood, as the spatial extent and nature of such regions can only be loosely inferred from standard magnetometry techniques. Currently, the state-of-the-art material for thin film read heads is CoFeB, which can exhibit perpendicular anisotropy when deposited on MgO.<sup>1</sup> Dead layers are known to be an issue for CoFeB,<sup>2</sup> as is B diffusion during annealing.<sup>3,4</sup> Several studies have shown that capping CoFeB with MgO minimizes the magnetic damage in the CoFeB.<sup>2,4-6</sup> Although much work has been done to minimize structural damage in CoFeB during etching,<sup>7-11</sup> the exact nature of the magnetic damage due to common etch methods is still unknown. With this in mind, we prepared a CoFeB sample with an etched surface and studied the structural and magnetic depth profiles with polarized neutron reflectometry (PNR) and cross-sectional transmission electron microscopy (TEM).

### II. EXPERIMENT

The sample was prepared by Seagate Technologies. A multilayer of Ta[5 nm]/MgO[1 nm]/CoFeB[10 nm] was

sputtered on an Si substrate capped with a 300 nm thermal oxide layer. Without exposing to atmosphere, 2 nm of the CoFeB was removed via low energy ion beam etching, after which the etched surface was capped with 5 nm of Cr. B-H loop measurements confirmed that the samples were ferromagnetic at room temperature, with coercive field less than 1 mT, and in-plane magnetic anisotropy. Such measurements of a series of identically structured samples with decreasing CoFeB thickness due to longer etch times showed a linear increase in saturation moment with thickness that imply a dead layer of approximately 1 nm.

Room temperature PNR measurements were conducted using the Polarized Beam Reflectometer (PBR) beamline at the NIST Center for Neutron Research. Neutrons of wavelength 0.475 nm were polarized to be spin-up (+) or spin-down (−) with respect to a 0.5 mT magnetic field applied in the plane of the sample. The non spin-flip specular reflectivities  $R^{++}$  and  $R^{--}$  of the samples were measured as a function of wavevector transfer,  $Q$ . Spin analysis was performed for the scattered beam, but no spin-flip scattering ( $R^{-+}$  and  $R^{+-}$ ) was detected. PNR is sensitive to the depth profiles of the nuclear composition and the in-plane component of the vector magnetization.<sup>12,13</sup>  $R^{++}(Q)$  and  $R^{--}(Q)$  are dependent on the sample's depth ( $z$ ) dependent scattering length density profile, which has nuclear and magnetic components

$$\rho^{\pm\pm}(z) = \rho_N \pm \rho_M. \quad (1)$$

The nuclear scattering length density is defined

$$\rho_N = \sum_i N_i b_i, \quad (2)$$

where  $b$  is the characteristic scattering length of a given isotope,<sup>14</sup>  $N$  is the number density of that isotope, and the summation  $i$  is over each isotope in the sample. The magnetic scattering length density is defined

$$\rho_M = CM, \quad (3)$$

<sup>a)</sup>Author to whom correspondence should be addressed. Electronic mail: brian.kirby@nist.gov.

where  $M$  is the magnetization, and  $C$  is a constant ( $C = 2.853 \times 10^{-7}$  for  $\rho_M$  in units of  $\text{nm}^{-2}$  and  $M$  in units of  $\text{kA m}^{-1}$ ). The spin-dependent reflectivities corresponding to a given scattering length density profile can be exactly calculated,<sup>12</sup> thus the profiles can be determined through model-fitting of the reflectivity data. For this work, modeling was performed using the ReFlID software package.<sup>15</sup> 2-sigma uncertainties for model parameters were determined using a Markov chain Monte Carlo analysis.<sup>15,16</sup>

Fitted PNR data for an etched sample are shown in Figure 1. Pronounced spin-dependent oscillations are observed over six orders of magnitude in reflectivity, indicating good sensitivity to nuclear and magnetic composition. X-ray reflectometry measurements (sensitive to the electron density depth profile) were also conducted. These measurements were consistent with the models used to fit the PNR data, but there was insufficient contrast among the surface layers of interest to add significant insight. Standard bright-field TEM measurements were conducted in a cross-sectional geometry, with an accelerating voltage of 300 kV. Contrast in the images shown is to first order proportional to atomic number and thickness.

### III. ANALYSIS

The depth profiles used to fit the Fig. 1 data are shown in Figure 2, plotted on top of a scaled cross-sectional TEM image of the sample. The PNR data could not be well fit using only the five layers described above ( $\text{SiO}_2$  thermal oxide, Ta seed, MgO buffer, CoFeB active layer, and Cr cap). However, by adding a surface layer corresponding to oxidized Cr, and by sub-dividing the CoFeB layer into fully magnetized region, and a non-magnetic, compositionally different etch-damaged region, we achieve an excellent fit to the data. (Note, although boron contributes both a real and imaginary component to the scattering length density,<sup>4</sup> best-fits to the data did not require a significant imaginary component, thus only the real component of  $\rho_N$  is shown in Fig. 2.) The nuclear profile shown in Fig. 2(a) shows excellent agreement with the TEM image. Starting from the  $\text{SiO}_2$  thermal layer, an uptick in  $\rho_N$  and dark image contrast are observed corresponding to the Ta seed, transitioning via a thin MgO layer into a higher  $\rho_N$  lighter TEM contrast region corresponding to amorphous CoFeB. This is followed by a step in  $\rho_N$  attributed to etch damage, and a lower  $\rho_N$  region with visible lattice fringes in the TEM image indicative of

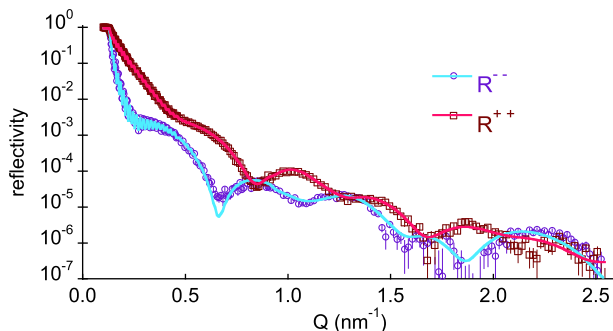


FIG. 1. Reflectivities for an etched sample in a 0.5 mT field. Lines are model fits to the data. Error bars correspond to  $\pm 1 - \sigma$ .

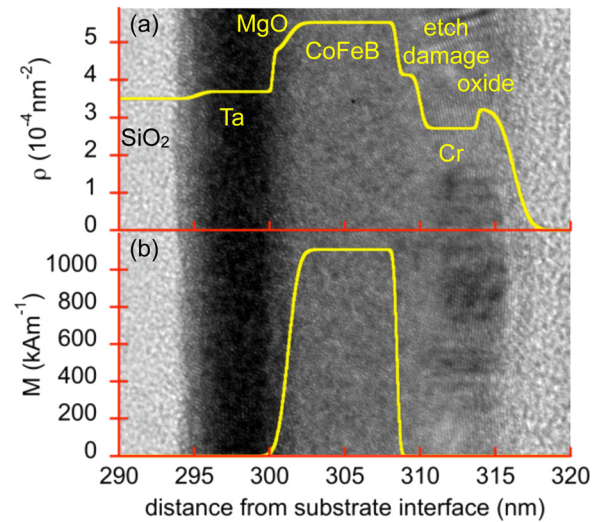


FIG. 2. Nuclear (a) and magnetic (b) depth profiles determined from the PNR data. The background is a scaled cross-sectional TEM image.

crystalline Cr. The compositional and structural nature of this 1.5 nm etch damage region is unclear, and invites further investigation. The TEM image shows a subtle change in contrast between the CoFeB and Cr, and the drop in  $\rho_N$  is attributable to either a change in isotopic composition or density (see Eq. (2)). In general, however, the agreement between measurement techniques lends significant credence to the PNR modeling results.

The corresponding magnetization profile is shown in Fig. 2(b) and is modeled as a uniform slab with equal magnetic and nuclear roughness at both the MgO/CoFeB and the CoFeB/etch damage interfaces. The best-fit value for the magnetized CoFeB thickness is  $7.2 \pm 0.03$  nm, with no magnetic dead layer due to the MgO/CoFeB interface. Since there is only one magnetized layer in the sample, and it is thick enough to produce distinct oscillations in the reflectivity, we are particularly sensitive to this total magnetized thickness. Thus, we observe a magnetized layer 10% thinner than expected, buried underneath a distinct  $1.5 \pm 0.1$  nm layer of non-magnetized material. This suggests that the etching induced dead layers implied by magnetometry originate from a significant change in composition at the etched CoFeB interface. Notably, the average rms roughness of the CoFeB/etch damage interface determined from PNR is only  $1.7 \pm 0.7$  nm, indicating the presence of a high quality, albeit buried, magnetic layer.

### IV. CONCLUSION

We have used PNR and TEM to characterize an ion beam etched CoFeB interface. We find that the total magnetized thickness is 10% thinner than the targeted CoFeB thickness, and that the magnetic layer is buried underneath a compositionally distinct, nonmagnetic damaged layer.

### ACKNOWLEDGMENTS

We thank Anusha Natarajathinam and Mark Kief of Seagate Technology for sample preparation and scientific

discussions, and thank Sandy Claggett of NIST for technical assistance. L.K. acknowledges support from the NIST SURF program, No. NSF DMR-0944772.

- <sup>1</sup>S. Ikeda, K. Miura, H. Yamamoto, K. Mizunuma, H. D. Gan, M. Endo, S. Kanai, J. Hayakawa, F. Matsukura, and H. Ohno, *Nature Mater.* **9**, 721 (2010).
- <sup>2</sup>S. Y. Jang, S. Lim, and S. Lee, *J. Appl. Phys.* **107**, 09C707 (2010).
- <sup>3</sup>J. J. Cha, J. C. Read, W. G. Egelhoff, P. Y. Huang, H. W. Tseng, Y. Li, R. A. Buhrman, and D. A. Muller, *Appl. Phys. Lett.* **95**, 032506 (2009).
- <sup>4</sup>T. Zhu, Y. Yang, R. Yu, H. Ambaye, V. Lauter, and J. Q. Xiao, *Appl. Phys. Lett.* **100**, 202406 (2012).
- <sup>5</sup>A. Natarajarathinam, Z. R. Tadisina, T. Mewes, S. Watts, E. Chen, and S. Gupta, *J. Appl. Phys.* **112**, 053909 (2012).
- <sup>6</sup>K. Oguz, P. Jivrajka, M. Venkatesan, G. Feng, and J. M. D. Coey, *J. Appl. Phys.* **103**, 07B526 (2008).
- <sup>7</sup>I. H. Lee, T. Lee, and C. Chung, *Vacuum* **97**, 49–54 (2013).
- <sup>8</sup>E. H. Kim, T. Y. Lee, B. C. Min, and C. W. Chung, *Thin Solid Films* **521**, 216 (2012).
- <sup>9</sup>Y. B. Xiao, E. H. Kim, S. M. Kong, and C. W. Chung, *Thin Solid Films* **519**, 6673 (2011).
- <sup>10</sup>J. Park, S. Kang, M. Jeon, M. Jhon, and G. Yeom, *J. Electrochem. Soc.* **158**, H1–H4 (2011).
- <sup>11</sup>K. B. Jung, H. Cho, Y. B. Hahn, D. C. Hays, T. Feng, Y. D. Park, J. R. Childress, and S. J. Pearton, *Mater. Sci. Eng., B* **60**, 101–106 (1999).
- <sup>12</sup>C. F. Majkrzak, K. V. O'Donovan, and N. F. Berk, in *Neutron Scattering from Magnetic Materials*, edited by T. Chatterji (Elsevier Science, New York, 2005).
- <sup>13</sup>M. R. Fitzsimmons and C. F. Majkrzak, "Application of polarized neutron reflectometry to studies of artificially structured magnetic materials," in *Modern Techniques for Characterizing Magnetic Materials*, edited by Y. Zhu (Springer US, New York, 2005) 10.1007/b101202.
- <sup>14</sup>I. S. Anderson, P. J. Brown, J. M. Carpenter, G. Lander, R. Pynn, J. M. Rowe, O. Scharpf, V. F. Sears, and B. T. M. Willis, *International Tables for Crystallography* (Wiley, Hoboken, New Jersey, New York, 2006), Chap. 4.4, p. 430.
- <sup>15</sup>B. J. Kirby, P. A. Kienzle, B. B. Maranville, N. F. Berk, J. Krycka, F. Heinrich, and C. F. Majkrzak, *Curr. Opin. Colloid Interface Sci.* **17**, 44 (2012).
- <sup>16</sup>J. A. Vrugt, C. J. F. T. Braak, C. G. H. Diks, D. Higdon, B. A. Robinson, and J. M. Hyman, *Int. J. Nonlinear Sci. Numer. Simul.* **10**, 273 (2009).